PARTICLE SHAPE DESCRIPTORS AND THEIR INFLUENCE ON THE MECHANICAL BEHAVIOR

Marie Chaze

PARTICLE SHAPE DESCRIPTORS AND THEIR INFLUENCE ON THE MECHANICAL BEHAVIOR

M. Chaze
LTDS, Ecole Centrale de Lyon, Université de Lyon1, 36 avenue Guy de Collongue, 69134 Ecully cedex, FRANCE
marie.chaze@ec-lyon.fr

ABSTRACT: *The present study is a part of a collaborative French national research project CEGEO/shape (Change of Scale in GEOmaterials). The purpose of benchmark collaborative numerical tests performed, using CD (Contact Dynamics) or MD (Molecular Dynamics) methods, is to quantify the non-circular shape of particles, by their degree of distortion relative to the disk, and to analyse their influence on the local and the macroscopic mechanical properties of granular materials. This contribution points out the compact collection of rigid octagonal shaped particles, built in accordance with our specific shape index. It also deals with the first investigations of realistic 3D particles. The following five biaxial compressions tests (which bring difficulties such as little deformations and multiple localizations) are numerical simulations, using NSCD (Non Smooth Contact Dynamic) method and LMGC90 software. The macroscopic behavior is studied in terms of solid fraction and internal angle of friction. We show that the internal angle is influenced by the increased anisotropy of friction forces and the contact orientations with the shape indicator. The variation of the initial assembly density (area of solids over total area) and the final density in the critical state is modelled using the number of particle edges, in order to explain the higher peak shearing resistance of assemblies with smaller initial void ratio or higher coordination number. Besides unilateral contact and Coulomb friction, other parameters relevant to the shape and contact anisotropy, which influence the anisotropy of stress transmission, as the ratio of edge-to-edge or vertex-to-edge active contacts, the stick-slip phenomenon, and the friction mobility, (ratio of tangential and normal contact forces) are quantified. Finally, different approaches have been proposed for the change of scale of kinematic variables. Analysis of local kinematics, and relation between the global strain and the local relative displacements at the contacts is studied.*

1 INTRODUCTION

Last decades, the discrete-element approach has been used as a tool to investigate the mechanical response of geomaterials at the grain level. Several averaging procedures have been proposed in order to define the stress and the strain tensor based on the contact forces and displacements of individual grains. These estimates have been used to perform a direct calculation of the incremental stress-strain response of disks and spheres assemblies. The modeling approach of DEM, especially with Coulomb friction criterion, is usually applied to clumps, by creating irregular curved composite particles. Since the spherical geometry of the particles overestimate the role of rotations, we should evaluate the incremental response by using arbitrary shaped particles. This DEM type simulation, which treat the particle as a

complex polygon was initiated by Favier et al. (1999), Alonso-Marroquin et al. (2005). Recently, some investigations appeared using three-dimensional loading paths with polyhedral particles, for example Latham J.P et al. (2008), Taylor et al. (2006).

2 BIDIMENSIONAL PARTICLE SHAPE DESCRIPTORS

The idea of our collaborative research project CEGEO, CECEO et al. (2010), is to propose a particle shape index, and to understand its role for the strength properties of the granular samples. Different 2D descriptors of shape can be extracted from the perimeter coordinates. Shape or form may be quantified from disk/sphere or from square/cube using surface area and/or volume comparison (spheres and cubes can be circumscribing into equivalent volume). It can also be quantified by axial ratios giving elongation or flatness Nouguier-Lehon (2010), Azema E. (2010). Another shape property governing both space filling and strength behavior, is the angularity or roundness. In our project we choose to vary the particle shape by their discrepancy or the degree of distortion from a circular particle (suggestion F. Radjai, LMGC). We characterized it using the scalar parameter:

$$\eta = \frac{\Delta R}{R}$$

where R is the radius of the largest circle containing the particle, and ΔR is the difference between the ex- and the in-circle of the particle. The present study is performed considering inscribed octagon, see Fig. 1. All the vertices are on the same circle of radius R, consequently the form is called isometric, and circumscribed in circle of radius R-ΔR, Chaze M. (2009).

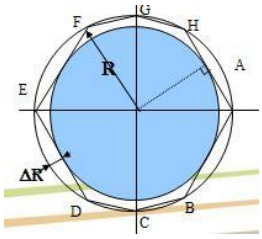

Fig. 1. Geometrical octagon design

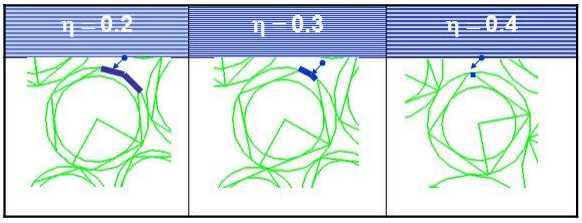

Fig. 2. Some typical octagons using the η evolution

These values are indeed within the intervals allowed by the construction, for example A_s° specific surface of the in-circle of octagon, (see Table 1).

3 THE 2D SAMPLES

The 2D granular model assembles 5000 poly-sized frictional particles. We generated five different samples of particles, varying η from 0. to 0.4 by step of 0.1, see Fig. 2 and 3. The octagonal particles were inscribed in the disks (radius R), which are the reference.

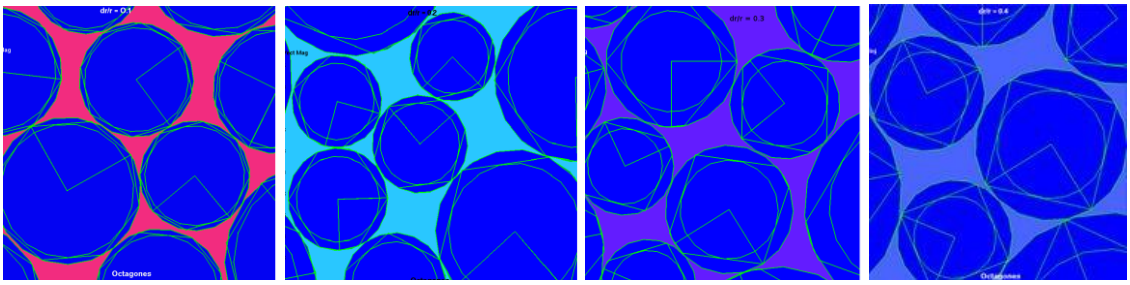

Fig. 3. Generation of different samples η = 0.1, 0.2, 0.3, 0.4

The method used for the creation of a sample is the follow: we begin with a dense packing composed of disks (η = 0), Voiret (2008), the reference, with a uniform distribution in particle volume fractions. The radius respects $R_{max} = 3R_{min}$, their ranges vary from $3.e^{-2}$ to 9.8 e^{-2} m and the density is equal to 2800 $kg.m^{-3}$. The orientation of particles is given by pseudo-random generator to reduce the preferential direction. We create a square sample, by applying a constant velocity on the right wall and on the upper wall. The initial velocity is randomized. This compaction procedure provides isotropic samples, and reduces the preferential direction of contact normal, (which does not occur if instead we use deposit under gravity). The interparticle friction is μ=0, for a dense confined packing and, the walls are frictionless. After that, the isotropic compression is computed by applying a constant stress**,** also called confining stress, 10 kPa, on the left, right and the upper wall. The isotropic samples were sheared by applying a displacement on the top wall and one constant confining stress on the lateral walls. To avoid dynamics effects, the velocity is chosen such as the *inertia parameter* $I \sim 10^{-4}$. The friction coefficient between grains is 0.5. The walls have masses equal approximately to the mass of the layer of grains, which has revealed to be a good choice the point of view of the dynamical response of the walls, with respect to the dynamical response of the grains.

4 THE NUMERICAL EXPERIMENTS

All simulations have been performed with the Open Source platform *LMGC90*, Dubois F. & Renouf M.(2006). http://www.lmgc.univ-montp2.fr/~dubois/LMGC90. The interaction laws use the *Contact Dynamics* approach which can treat unilateral and dry friction without smoothing approximation. We should reconsider the Signorini complementary condition, Jean M. (1999). The model used in these hereafter experiments, the IQS (Inelastic Quasi Shock) frictional contact law, is treated with NSCD method (an implicit scheme using large time steps), Cambou B. & Jean M. (2001). The computation has been performed with the same parameters, for the five benchmark tests except for the maximal number of iterations, especially during the peak in order not to deteriorate the equilibrium results.

5 MECHANICAL ANALYSIS OF THE TESTS MICROSCOPIC RESPONSE

The following figures present evolution of the samples microscopic response at the initial and critical states:

in initial isotropic state

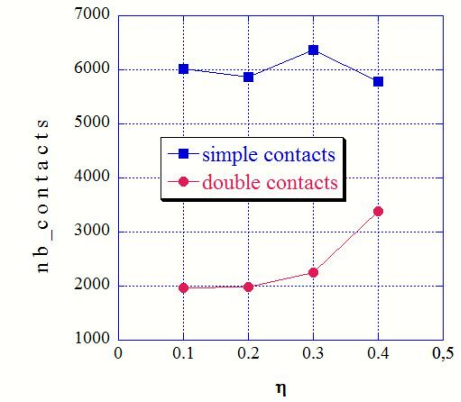

in critical state

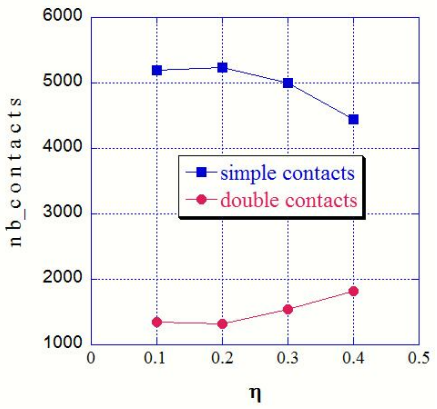

Fig. 4. Evolution of the contacts number with η at initial isotropic and critical states

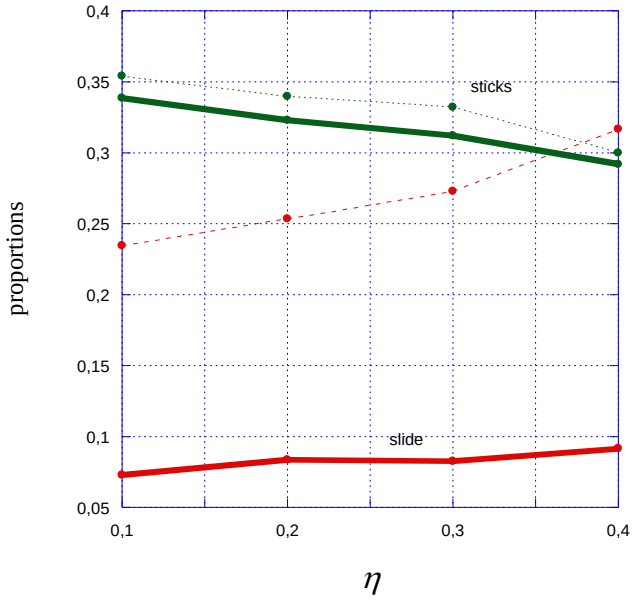

Fig.5. Evolution of stick (edge-to-edge) and slide (vertex-to-edge) contacts in the strong (plain line) and weak (dashed line) networks as a function of η in the residual state

Fig. 4. and Fig. 5. provide evidence for large class of "weak" forces carried by vertex-to-edge slide contacts. Strong force chains are composed of edge-to-edge stick contacts. We also observe that the proportion of double contact, side-to-side contact increases with η both in initial isotropic and in critical states (especially for $\eta \geq 0.4$ when the octagons became squares result of the occurrence of facetization). Numerical studies have allowed to identify two contact network. The strong network consisting primarily of stick contacts, acts as the skeleton du milieu. Efforts are essentially propagated through it. The weak network, composed essentially of slide contacts, is more unstable.

Similar tendency with contact coordination number Z_{iso}, defined as the mean number of contacts per particle in initial isotropic state and, Z_{critic} in critical state. We distinguish the coordination number $Z^{'}$ (see Table 2) as the mean number of contacting neighbors per particles, from the Z defined as the mean number of contacts per particle, Fig. 6. $Z_{iso}^{'}$ may be correlated with the number of particle's degrees of freedom and, consequently, they take place in the mechanical equilibrium of particles CEGEO et al. (2010).

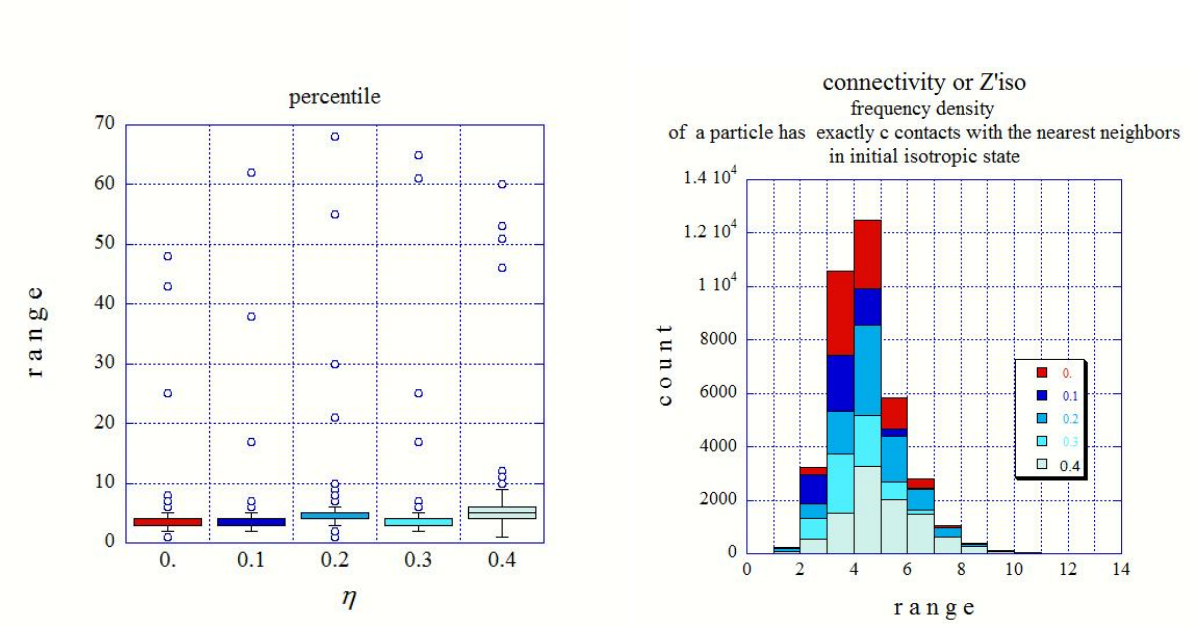

Fig. 6. Percentile rank and histogram of distribution of a dataset Z'_{iso} as a function of η

Shapes indicator	0.	0.1	0.2	0.3	0.4
Coordinence Z_{iso}' Z_{critic}'	3.81 3.116	5.01 3.24	5.90 **3.36**	5.20 **3.7**	5.01 3.69
Compacity C_{iso} C_{crit}	0.845-0.81	0.851-0.784	0.859-0.80 0.863-0.802 0.8629-0.792	0.874-0.815 0.8739-0.8026	0.876-0.820 0.8759-0.8089

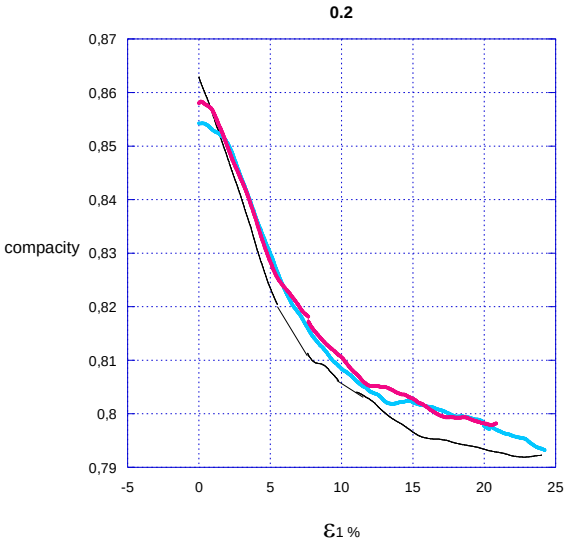

Percentiles represent the summation or integral of the area under the normal curve. Box plot: the horizontal line in the center indicates the median (50th percentile), top and bottom, 25th and 75th. For example, when $\eta = 0.$ we deduce, in Fig. 6., that the median is around four and the half of grains has a connectivity of about four. The points which are out of the box

represent the number of contacts with the wall. An interesting feature of the histogram graph is that, the proportion of c contact number of a particle with its nearest neighbors, is maximum to the class [4,5] for the non-circular particles. The sample is prepared with μ = 0.

The texture of two packings η 0.3 and 0.4 in terms of normal contact distribution is present Fig. 8. and 9. The privileged direction rotates as a result of vertical compression and becomes vertical in the residual state.

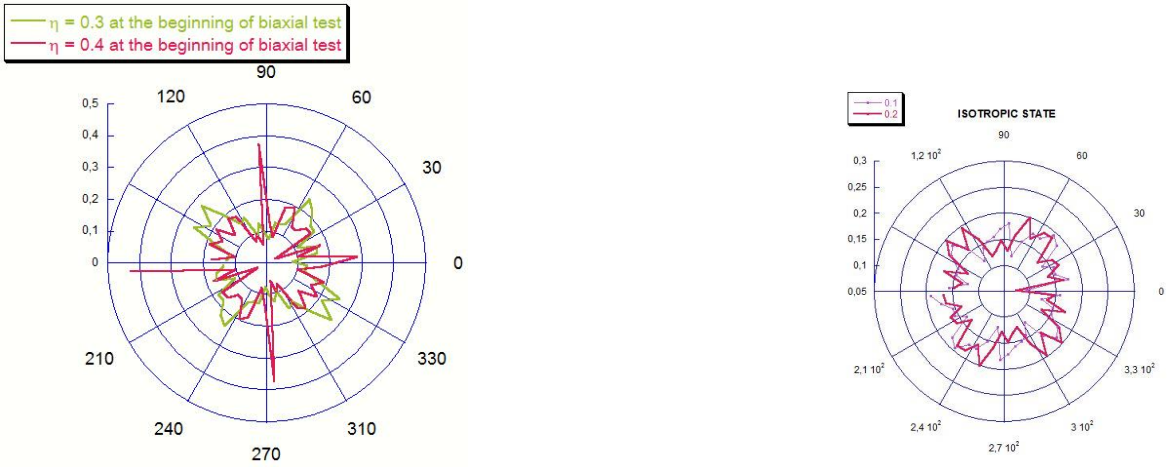

Fig. 8. Polar representation θ of normal conctact distribution normalized, for $\eta = 0.3$ and 0.4 at the beginning and the critical state

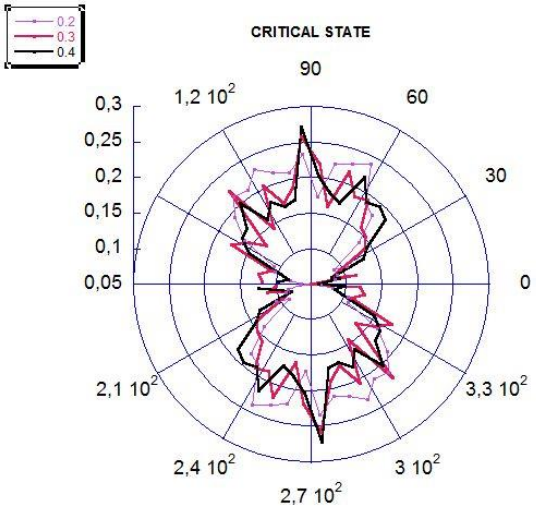

Fig 9. Polar representation θ of normal conctact distribution normalized, for $\eta = 0.2$ 0.3 and 0.4 at the beginning and the critical state

6 MECHANICAL ANALYSIS MACROSCOPIC RESPONSE OF THE TESTS

In Fig. 10. the dilation response of the sample containing octagons shows steeper dilatancy slope than the assembly containing disks. Squares show steeper dilatancy slope than octagons.

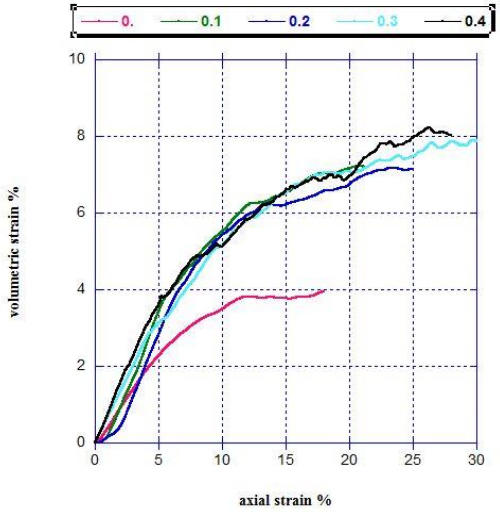

Fig. 10. Volumetric strain versus axial strain

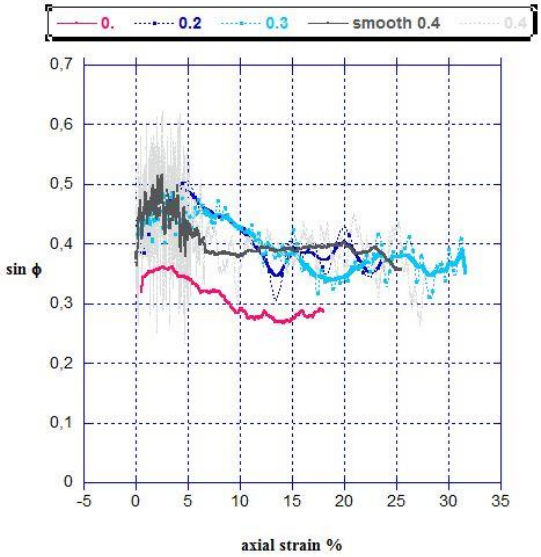

Fig. 11. Stress Strain response

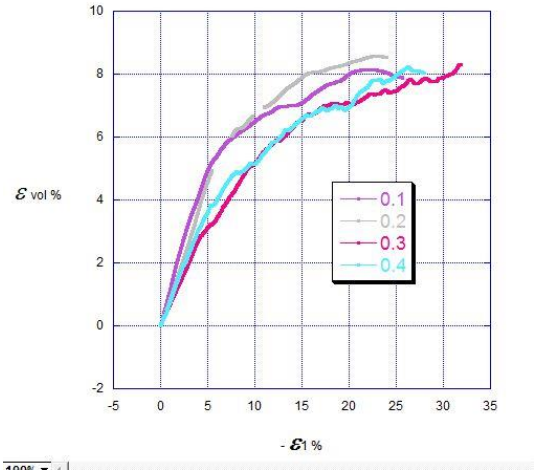

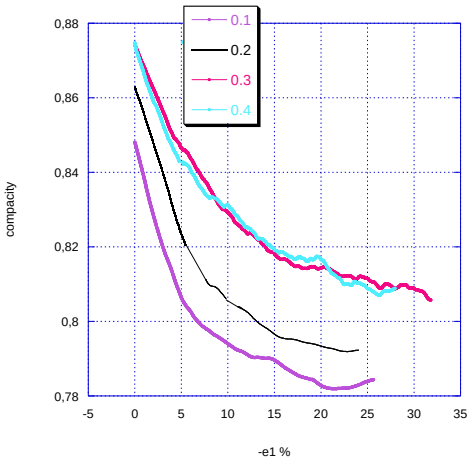

Fig. 10bis. Volumetric strain and compacity versus axial strain for octagons assemblies (η = 0.1, 0.2, 0.3, 04)

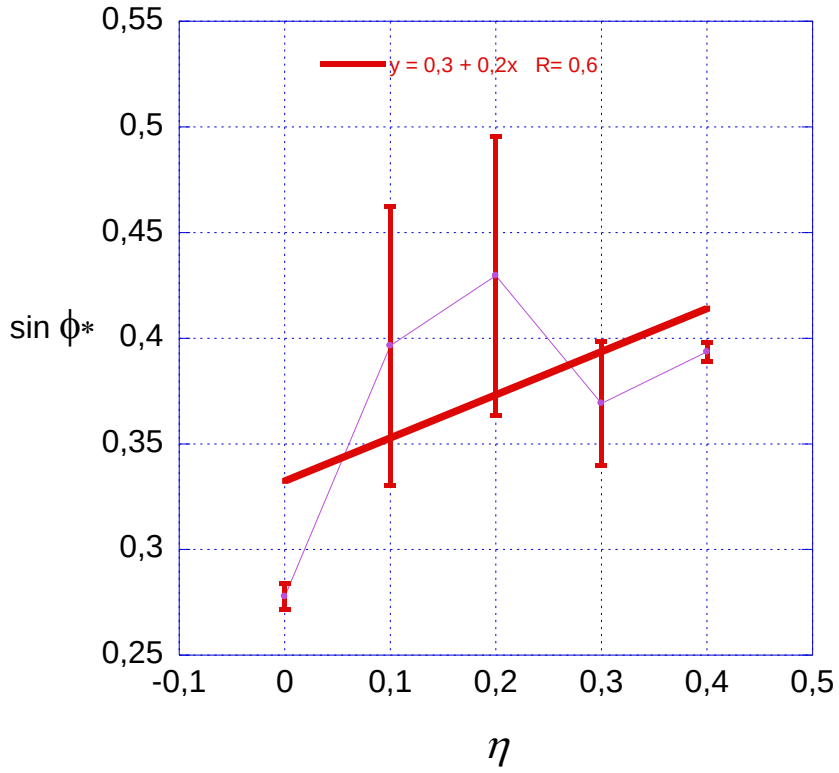

Fig. 11. sin ϕ^* versus η

The shear strength is characterized by the internal angle of friction ϕ, such the sin ϕ= q / p, where q = $(\sigma_1 - \sigma_2)/2$ and p = $(\sigma_1+\sigma_2)/2$. The sin ϕ increases from zero to a peak value and after is relaxing to a constant material-dependents value sin ϕ^*. Fig.11 seems to indicate that sin ϕ^* increase with η.

We define a static quantity, CEGEO et al. (2010),

$$M = < \frac{f_t}{(\mu f_n)} > \qquad (3)$$

where f_t is the absolute value of the friction force, f_n is the normal force. Fig. 12. shows that the rotational degrees of freedom, M, is an increasing function of η.

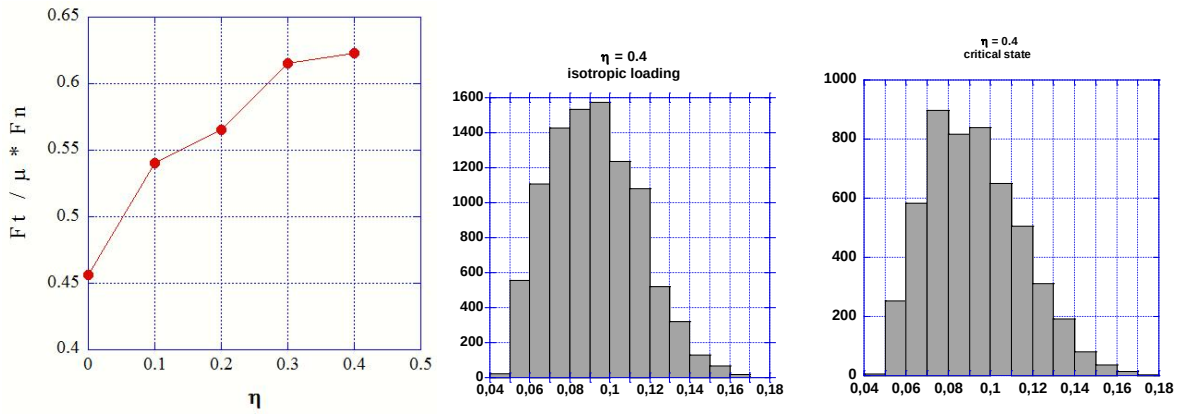

Fig. 12. Friction mobilization in the steady state as a function of η

Fig. 13. Distribution of branch vector set for η = 0.4 in initial isotropic and critical states

7 ANALYSIS OF LOCAL KINEMATICS

In unconsolidated granular media an important element is the description of local arrangement of the grains and the possible correlations between their positions. The simplest way of describing neighborhood and the steric environment of a grain is to build its Voronoi cell, to study its size and shape, and to correlate them with the nearest neighbors. Here we calculate branch vector, Konishi et al. (1988), as the vector connecting two particles in contact.

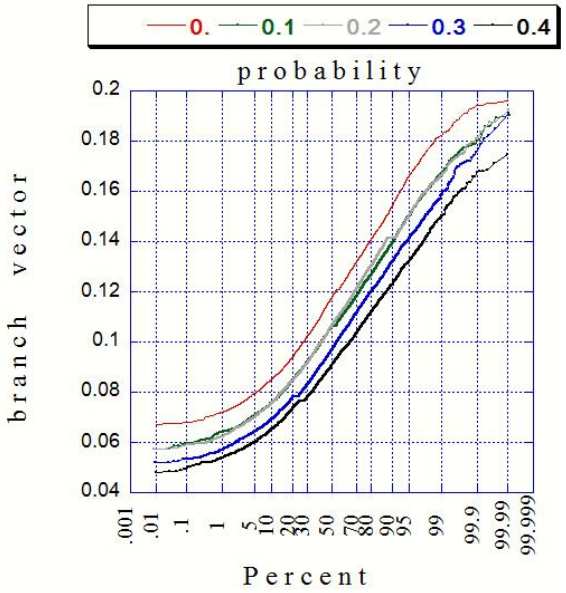

Fig. 14. Probability distribution function of branch vector set for the different value of η

The distribution of branch vector, Fig. 14, confirms the previous results of the assemblies with smaller initial void ratio or higher coordination number. To establish the link between local variables, the void ratio and the strain tensor we apply the relationship between local displacements of particles and the strain tensor, Cambou, Chaze et al. (2000). The incremental strain is defined "Eq. 4", respect to hypothesis of small strains, with the reference configuration defined at the beginning of the analyzed increment, so:

$$\delta\varepsilon_{ij}^{\alpha} = \frac{1}{2}\left(\frac{\delta u_i^{\alpha}}{\delta x_j^{\alpha 0}} + \frac{\delta u_j^{\alpha}}{\delta x_i^{\alpha 0}}\right) \tag{4}$$

where $\delta\varepsilon_{ij}^{\alpha}$ is the increment of strain defined for α increment, δu_i^{α} is the increment of displacement during α increment, $x_i^{\alpha 0}$ is the reference configuration defined at the beginning for α increment. Using the Delaunay triangulation it will be possible to derive a mean value of the global strain and it is assumed that the strain tensor defined on each triangular element is constant.

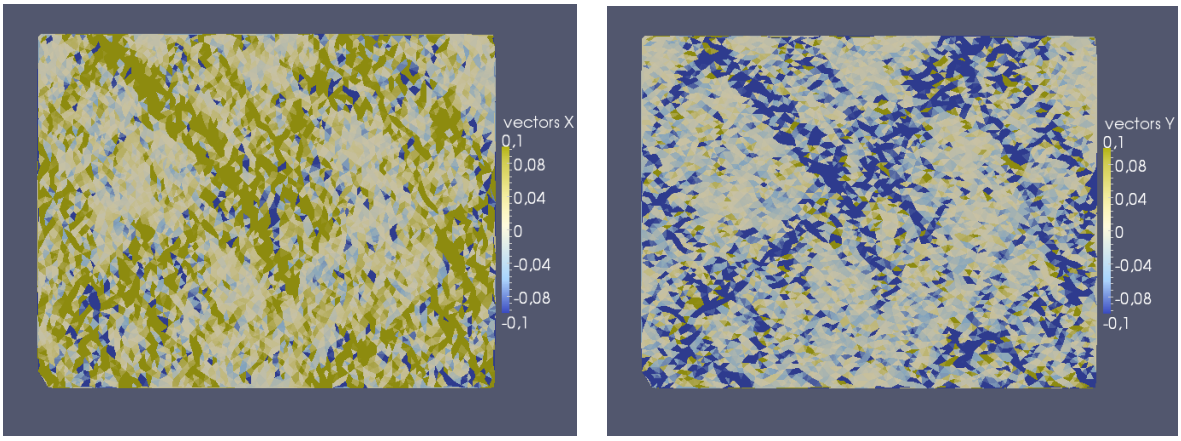

Fig. 15. View of ε_{11} for compressive displacement and ε_{22} for extension displacement for η = 0.3 near the peak value of the internal angle of friction .

Different deformation regimes may be expected: at the beginning of the compression the deformation is much more distributed Fig. 16 and, as show in Fig. 15 shear band have been developed. In the critical state the shear bands are missing, Fig. 17. For both figures the density contrasts are similar.

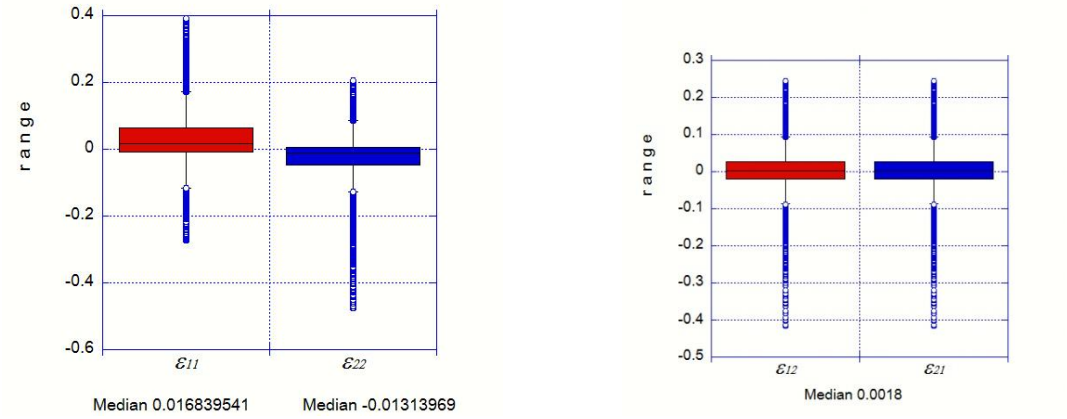

Fig. 16. Percentile of a dataset ε_{11}, ε_{22}, ε_{12}, ε_{21} according to deformation's definition

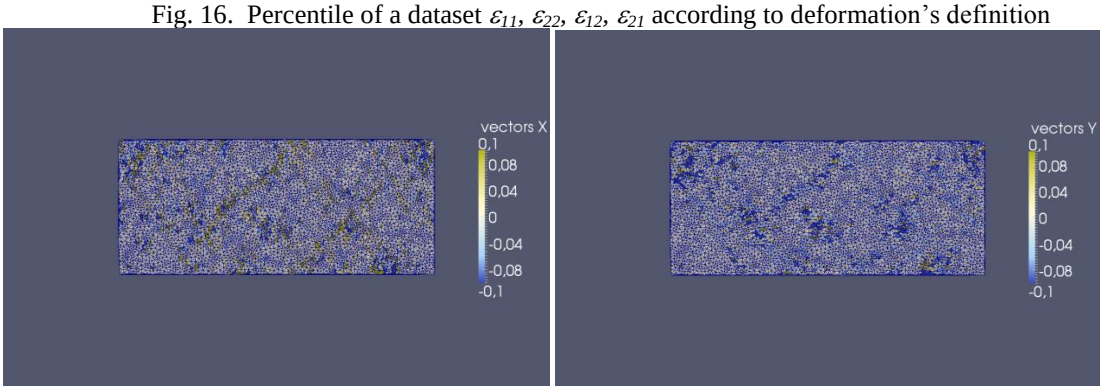

Fig. 17. Repartition of ε_{11} and ε_{22} resulting between 0.1 % increment of strain in the critical state.

To measure the localization of deformation Davy at al. (1995), use a participation ratio defined as:

$$S = \frac{1}{\Sigma} \frac{\left(\iint_{\Sigma} \varepsilon \mathrm{d}S\right)^2}{\iint_{\Sigma} \varepsilon^2 \mathrm{d}S}, \tag{5}$$

ε represents a scalar measure of the deformation tensor, Σ is the surface area. The participation ratio Σ is a measure of the percentage surface that appears deformed. If ε is perfectly homogeneously distributed Σ equal 1. As deformation becomes localized, Σ is smaller than 1; the larger the fluctuations become in local strain, smaller is Σ. If the deformation is localized in a shear band, Σ is a measurement of the surface of this shear band. These calculations provide a physical framework to understand the role of disorder and local deformation mecanisms on the deformation processes.

8 3D EXTENSION

To go further, we model 3D shape effects in granular systems. We started with the sample composed of polyhedral particles, which have the following specifications: average vertex number 10, vertex total number 9960, average face number 16, number of total faces 15936. The first results, are showing in Fig. 18 and 19, are promising and realistic.

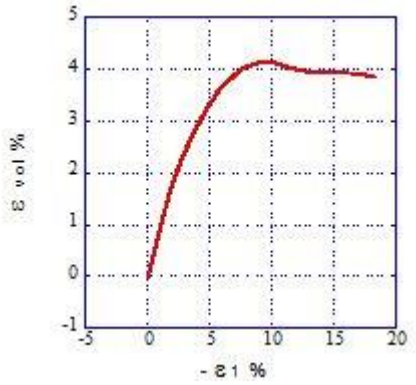

Fig. 18. Volumetric strain versus axial strain

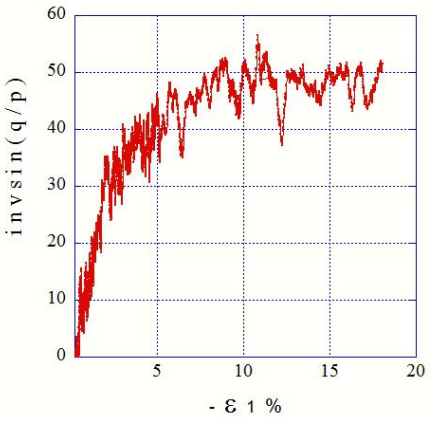

Fig. 19. Stress Strain response

9 CONCLUSION

The goal in these experiments is to suggest that the use of shape parameter η, describing deviation to circular shape applied to the isometric octagons, enforces and controls certain mechanically based rules of granular media. The doctrine that these samples present some difficulties does not prevent to demonstrate that the shear strength has a monotonic dependence to η. With the variation of η, octagons become irregular, regular, and square with change of vertex number. Besides unilateral contact and Coulomb friction, the change of vertex number influences the ways of contacting, vertex against side, side against side, and also the friction mobilization. Such contacts cause severe *indetermination*, i.e. the contact forces solution of the dynamical problem, is far to be unique, due the rigid behavior of the grains, and to Coulomb friction. Also, *locking* may happen, the evolution of the grains is not possible or is possible only if the reaction forces increase dramatically, and in rough case, if at last some errors are allowed. These behaviors are favored in collections of octagons which have a tendency to organize as crystals, like clusters, while collections of poly-sized disks are easier to deform.

ACKNOWLEDGEMENT

The author is indebted Danescu A., Cambou B., Radjai F., Jean M. for theirs stimulations, Dubois F. and Renouf M., the authors of the *LMGC90* software, for many remarks.

REFERENCES

Alonzo-Marroquin, F., & Hermann, H.J., (2005) "The incremental response of soil. An investigation using a discrete-element model", Journal of Engineering Mathematics 52, 11-34.

Azéma, E., & Radjaï, F., (2010) "Stress-strain behavior and geometrical properties of packings of elongated particles", Phys. Rev. E **81**, 051304.

Cambou, B., & Chaze, M., & Dedecker. F., "Change of scale in granular materials", Eur. J. Mech. A/Solids 19(200) 999-1014.

Cambou, B., & Jean, M., (2001), Micromécanique des matériaux granulaires, Hermes Sciences, Traité MIM.

Chaze, M., (2009), "Effect of grain shape on the behaviour of granular materials in biaxial compression", Proceedings of '2009 COMGEO, France, International Center for Computational Engineering-eJournal.

CEGEO, Saint-Cyr, & Szarf, & Voiret, & Azema, & Richefeu, & Delenne, & Combe, & Nouguier-Lehon, & Villard, & Sornay, & Chaze, & Radjai, (2010), "Particle shape dependence in granular media" submitted PRL.

Davy, P., & Hansen, A., & Bonnet, E., & Shou-Zhu Zhang, (1995) "Localization and fault growth in layered bittrle-ductile systems: implications for deformations of the continental lithosphere", JOURNAL OF GEOPHYSICAL RESEARCH, VOL. 100, NO. B4, PAGES 6281-6294, APRIL 10.

Dubois, F. & Renouf, M. (2007), "Numerical strategies and software architecture dedicated to the modeling of dynamical systems in interaction. Application to multibody dynamics". MULTIBODY DYNAMICS 2007 Thematic Conference Milano, Italy.

Favier, J.P., et al. (1999), "Shape representation of axi-symetrical, non spherical particles in discrete element simulation using multi-element particles", Engineering Computation 16(4), 467-480.

Jean, M., (1999), "The non smooth contact dynamics method" Comp. Meth. Appl. Mech. Engrg. Vol 177, 233-257.

Konishi, J., Narusi F., (1988), "A note on fabric in terms of voids", Micromechanics of Granular Materials, edited by Satake M.

Latham, J.P., & Munjiza, A., & Garzia, X., &Xiang J., & Guises, R., (2008) "Three-dimentional particle shape acquisition and shape library for DEM and FEM/DEM simulation*"* Mineral Engineering 21, 797-805

Nouguier-Lehon, C., (2010), "Effect of the grain elongation on the behavior of granular materials in biaxial compression*"*, C. R. Mécanique 338, pp. 587-595.

Voiret, C. (2008) Ph.D. thesis, Université Montpellier II.

Taylor, M.A., Garboczi, E.J., Erdogan, S.T., Fowler, D.W., 2006, "Some properties of irregular particles in 3D, Powder Technology 162, 1-15.